Journal of Sound and Vibration (1999) **220**(3), 383–411
Article No. jsvi.1998.1917, available online at http://www.idealibrary.com on IDEAL

THE NON-LINEAR SLOW NORMAL MODE AND STOCHASTICITY IN THE DYNAMICS OF A CONSERVATIVE FLEXIBLE ROD/PENDULUM CONFIGURATION

I. T. GEORGIOU* AND I. B. SCHWARTZ
Naval Research Laboratory, *Washington*, *DC* 20375, *U.S.A.*

(*Received* 13 *March* 1997, *and in final form* 31 *July* 1998)

The geometric structure has been analyzed of the slow periodic motions of a conservative structural/mechanical system consisting of a stiff linear elastic rod coupled to a non-linear pendulum oscillator. Using the theory of geometric singular perturbations, we have computed analytically a two-dimensional invariant non-linear manifold of motion in phase space, called the slow manifold. Numerical experiments reveal that all motions initiated on the slow manifold are purely slow periodic and share common properties. The slow invariant manifold is the geometric realization of a non-linear normal mode, which consists of master and slaved dynamics. The normal mode is non-classical since it does not satisfy the classical definition of vibrations-in-unison. The analysis reveals that the slow invariant manifold carries a heteroclinic motion. Its existence is verified numerically by showing that all its Lyapunov characteristic exponents are zero. Above some critical coupling between the flexible rod and pendulum, the slow normal mode interacts, first at the energy level of the heteroclinic motion, with the fast dynamics to create stochastic motions. The strength of stochasticity, measured by the Lyapunov characteristic exponents, increases as the coupling increases.

1. INTRODUCTION

Coupled structural/mechanical systems such as robots, tethered spacecrafts, rotating shafts supporting multiple disks, and ship cranes, to name a few, involve coupling between stiff (high natural frequencies) linear or weakly non-linear continuous structures and soft (low natural frequencies) non-linear oscillators. A pendulum coupled to a stiff elastic rod is an example of such a soft/stiff system of infinite degrees of freedom. In modelling such structures, is has been assumed in the past that the stiff substructure does not affect the dynamics of the soft substructure. The objective of this paper is twofold. First, the flexible rod/pendulum system is used as a prototype to develop a systematic methodology to study large scale multi-degree-of-freedom soft/stiff systems. Second, and most important, it is shown how the dynamics of the pendulum oscillator are modified

* Currently a Research Scientist with SAIC, McLean, VA 22102, U.S.A.

0022–460X/99/080383 + 29 $30.00/0

when the latter is coupled to a linear elastic continuum. The pendulum oscillator has been the subject of numerous studies in physics and engineering [1–6]. In non-linear dynamics studies, it is one of the most common, along with the Duffing oscillator, used one-degree-of-freedom non-linear systems to demonstrate various features of non-linear dynamics such as the period doubling bifurcation route to chaos and solitons [5, 6]. It is thus natural and challenging to explore how the dynamics of this well studied one-degree-of-freedom system are modified when coupled to continuum structural systems. In this work, the focus is on characterizing the invariant geometric objects in phase space of the conservative pendulum/flexible rod system. In particular, it is shown that the phase space contains a global non-linear invariant manifold. This manifold is two-dimensional and it consists of a family of purely slow, orbitally stable, periodic motions. The dynamics restricted on the slow manifold are governed by a non-linear oscillator with a phase portrait qualitatively the same as that of the pendulum. This non-linear oscillator slaves the stiff rod into slow periodic motions. Above some critical coupling and at the unstable equilibrium energy level, stochasticity develops for the first time. As the coupling increases stochasticity appears at lower energy levels and it diffuses into large regions of the phase space.

2. FLEXIBLE ROD/PENDULUM SYSTEM

Figure 1 depicts a structural/mechanical system consisting of a vertical flexible rod of length L and cross-section A supporting at its lower end A a non-linear pendulum of length L_p and mass M_p. The pendulum is restricted to move only in one plane whereas the rod free end O is fixed. The rod is made of linear elastic material of modulus E and mass density ρ. The constant g denotes the gravitational acceleration.

Let x denote the co-ordinate of the cross-section A when the rod is uncoupled and unloaded. The displacement field $u(x, t)$ of the rod and the angular displacement $\theta(t)$ of the pendulum will be referred to co-ordinate axes fixed at the rod ends O and A, respectively. Let $u_A(t)$, and $\ddot{u}_A(t)$ denote the displacement and acceleration of the rod end A. The motion then of the rod/pendulum system is described by the following set of equations:

$$\ddot{\theta} + \left[\frac{g}{L_p} - \frac{\ddot{u}_A(t)}{L_p}\right] \sin(\theta) = 0, \qquad \ddot{u}(x, t) - \frac{E}{\rho} u''(x, t) = \frac{g}{\rho}, \tag{1a, b}$$

$$u(x = 0, t) = 0, \qquad AEu'(x = L, t) = T_p \cos(\theta), \tag{1c, d}$$

where $(\dot{})$ and $(')$ denote partial differentiation with respect to time t and space x, respectively. The term T_p denotes the tension along the rigid pendulum arm and is given by $T_p = M_p L_p \dot{\theta}^2 + M_p[g - \ddot{u}_A(t)] \cos(\theta)$. The motions of the pendulum (1a) is coupled to the motion of the rod (1b) through the boundary condition (1d).

The coupled ODE/PDE nonlinear system (1) is normalized by introducing the dimensionless space and time variables $\xi = x/L$, $\tau = \omega_p t$; the dimensionless displacement $U = u/L_p$; and the following frequency and mass ratios: $\mu = \omega_p/\omega_1$,

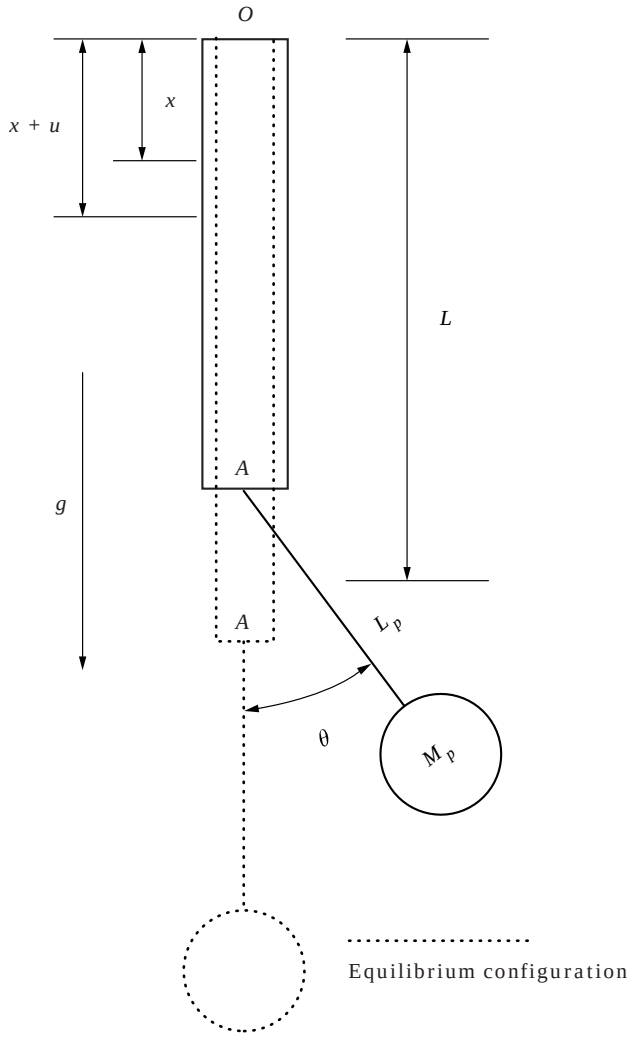

Figure 1. A flexible rod/pendulum configuration.

$\mu_m = \omega_1/\omega_m$, $\beta = M_p/A\rho L$, where $\omega_p^2 = g/L_p$, $\omega_m^2 = \pi^2(2m-1)^2/L^2 \times E/\rho$, $m = 1, 2, \ldots$, are the natural frequencies of the pendulum and uncoupled flexible rod, respectively.

The equilibrium configurations of the coupled system are given by

$$C \equiv (\hat{\theta} = 0,\ \hat{U}(\xi)), \qquad S_{\pm 1} \equiv (\hat{\theta} = \pm\pi,\ \hat{U}(\xi)), \tag{2}$$

where $8\hat{U}(\xi) = \mu^2\pi^2[2(1+\beta)\xi - \xi^2]$ denotes the static displacement field of the rod due to the combined action of the pendulum weight and gravity. Let $V(\xi, \tau)$ denote the displacement with respect to the stable equilibrium configuration C, i.e., $U(\xi, t) = \hat{U}(\xi) + V(\xi, \tau)$. The normalized equations of motion are given by

$$\ddot{\theta} + [1 - \ddot{V}_A(\tau)] \sin(\theta) = 0, \qquad \mu^2\pi^2\ddot{V}(\xi, \tau) - 4V''(\xi, \tau) = 0, \tag{3a, b}$$

$$V(\xi = 0, \tau) = 0, \qquad 4V'(\xi = 1, \tau) = -\mu^2\beta\pi^2[1 - T\cos(\theta)], \tag{3c, d}$$

where $T \equiv T_p/M_pL_p\omega_p^2 = \theta^2 + [1 - \ddot{V}_A]\cos(\theta)$ denotes the normalized pendulum tension.

Equation (3b) and the boundary condition (3d) reveal that the frequency ratio μ and the mass ratio β measure the strength of coupling between the pendulum substructure and the flexible rod substructure. The coupling parameters can assume values equal to or greater than zero.

For fixed ratio β, the limit of coupled system (3) as $\mu \to 0$ yields

$$\ddot{\theta} + \sin(\theta) = 0, \qquad V(\xi, \tau) = 0. \tag{4, 5}$$

This is the equation of motion of the uncoupled pendulum supported by a perfectly *rigid* rod. On the other hand, if the time scale τ is scaled to the fast time scale $\tau_1 = \tau/\mu$ and the limit of (3) is taken as $\mu \to 0$, one obtains the following equations:

$$\ddot{\theta} = 0, \qquad \pi^2 \ddot{V}(\xi, \tau_1) - 4V''(\xi, \tau_1) = 0, \tag{6a, b}$$

$$V(\xi = 0, \tau_1) = 0, \qquad V'(\xi = 1, \tau_1) = 0. \tag{6c, d}$$

Now $(\dot{})$ denotes differentiation with respect to the fast time τ_1. This is the equation of motion of the uncoupled flexible rod. We are interested in the dynamics of the coupled system for small coupling μ. One interesting consequence of the limiting process is the reduction of dimension of the dynamics. In view of the limiting systems, we ask *how are the dynamics of the coupled system related, if at all, to the dynamics of the uncoupled soft subsystem* (4) *and uncoupled stiff subsystem* (6)? We will apply the geometric singular perturbation (GSP) theory [7–9] to study the dynamics of the coupled system. The GSP approach to study coupled dynamical problems in mechanics has been used to study two- and three-degree-of-freedom systems [10–13].

3. GEOMETRIC SINGULAR PERTURBATION FORMULATION

In Appendix A a model decomposition is performed to transform the coupled ODE/PDE system (3) into the following infinite set of coupled oscillators:

$$\ddot{\theta} + \left[1 - \sum_{m=1}^{N} (-1)^{m+1} \ddot{\eta}_m\right] \sin(\theta) = 0, \tag{7a}$$

$$\sum_{j=1}^{N} L_{mj}(\theta)\ddot{\eta}_j + \frac{\eta_m}{\mu^2\mu_m^2} + (-1)^{m+1} 2\beta[\sin^2(\theta) - \dot{\theta}^2 \cos(\theta)] = 0, \tag{7b}$$

where $L_{mj}(\theta) \equiv \delta_{mj} + (-1)^{m+j+2} 2\beta \cos^2(\theta)$; $m, j = 1, 2, 3, \ldots, N \to \infty$, and where δ_{mj} denotes an element of the Kronecker delta. For fixed N, equation (7b) can be solved for the modal inertias $\ddot{\eta}_m$.

Now the linear transformation

$$\theta = \Psi_1, \qquad \dot{\theta} = \Psi_2, \qquad \eta_m = \mu^2 \mu_m^2 Z_{2m-1}, \qquad \dot{\eta}_m = \mu \mu_m^2 Z_{2m}, \tag{8}$$

casts coupled oscillators (7) into the following set of first order differential equations:

$$\dot{\Psi}_1 = \Psi_2,$$

$$I_N(\Psi_1)\dot{\Psi}_2 = -\left[1 + 2\beta N(1 - \Psi_2^2 \cos(\Psi_1)) + \sum_{j=1}^{N} (-1)^{j+1} Z_{2j-1}\right] \sin(\Psi_1), \tag{9a}$$

$$\mu \dot{Z}_{2m-1} = Z_{2m},$$

$$\mu \mu_m^2 I_N(\Psi_1)\dot{Z}_{2m} = -I_{N-1}(\Psi_1) Z_{2m-1} + 2\beta \cos^2(\Psi_1) \sum_{j=1, j\neq m}^{N} (-1)^{m+j+2} Z_{2j-1}$$

$$+ (-1)^{m+1} 2\beta [\Psi_2^2 \cos(\Psi_1) - \sin^2(\Psi_1)], \tag{9b}$$

where $I_N(\Psi_1) \equiv 1 + 2\beta N \cos^2(\Psi_1) \neq 0$ and $m = 1, 2, \ldots, N \to \infty$. The equilibrium states of coupled oscillators (9) are

$$C \equiv (\{\hat{\Psi}_1, \hat{\Psi}_2\}, \{\hat{Z}_1, \hat{Z}_2\}, \ldots, \{\hat{Z}_{2N-1}, \hat{Z}_{2N}\}) = (\{0, 0\}, \{0, 0\}, \ldots, \{0, 0\}),$$

$$S_{\pm 1} \equiv (\{\hat{\Psi}_1, \hat{\Psi}_2\}, \{\hat{Z}_1, \hat{Z}_2\}, \ldots, \{\hat{Z}_{2N-1}, \hat{Z}_{2N}\}) = (\{\pm\pi, 0\}, \{0, 0\}, \ldots, \{0, 0\}).$$

Equilibrium C is a center whereas $S_{\pm 1}$ are saddle-centers, their energy levels being $E_\mu(C) = 0$, $E_\mu(S_{\pm 1}) = 4\beta$. They are the discrete analogues in phase space now of the equilibrium configurations (2).

Equation (9) represents the original equations of motion (3) as a *singular perturbation* of the uncoupled pendulum. The frequency ratio μ plays the role of the *singular* perturbation parameter and, for fixed mass ratio β, measures the strength of coupling between the pendulum and the flexible rod. For small coupling μ, fixed mass ratio β, the dynamics evolve on a slow time scale τ and the ordered sequence of fast time scales $\{\tau/\mu, 3\tau/\mu, 5\tau/\mu, \ldots, (2m-1)\tau/\mu, \ldots\}$. The singular perturbation formulation brings out clearly the hierarchy of time scales.

For convenience and effective implementation of symbolic computations that will follow later, coupled oscillators (9) are written in the following compact format:

$$\dot{\Psi} = \mathbf{F}(\Psi; N) + \mathbf{A}(\Psi; N) Z, \tag{10a}$$

$$\mu \dot{Z} = \mathbf{B}(\Psi; N) Z + \mathbf{G}(\Psi; N), \qquad N \to \infty, \tag{10b}$$

where $\Psi \equiv (\Psi_1, \Psi_2)$, and $Z \equiv (\{Z_1, Z_2\}, \{Z_3, Z_4\}, \ldots, \{Z_{2N-1}, Z_{2N}\})$. The terms $\mathbf{F}$, $\mathbf{A}$, $\mathbf{B}$, $\mathbf{G}$ are non-linear functions of Ψ. The inverse of the $2N \times 2N$ matrix $\mathbf{B}$ exists for all Ψ and N. For small μ, we call Ψ and Z the slow and fast variable, respectively. Note that the singular perturbation formulation of the equations of motion is valid for any admissible value of μ.

4. REDUCED DYNAMICS

We seek all motions of the coupled system that evolve on the slow time scale of the uncoupled pendulum. Recall that its natural frequency is normalized at $\omega_p = 1$. To tackle this issue, a two-dimensional invariant manifold is required. A manifold is invariant if any motion initiated on it remains on it for all time. The singular perturbation formulation introduces naturally geometry in the form of invariant manifolds, which in turn address the issue of dimension reduction. For fixed mass ratio β, the limit, as $\mu \to 0$, of the equation of motion of the stiff rod (10b) is the algebraic equation

$$0 = \mathbf{B}(\Psi; N)Z + \mathbf{G}(\Psi; N), \tag{11}$$

its solution being

$$Z = \mathbf{H}^0(\Psi; N) = -\mathbf{B}^{-1}(\Psi; N)\mathbf{G}(\Psi; N). \tag{12}$$

The explicit expression of the mth pair element of the vector-valued function $\mathbf{H}^0$ is given by

$$\begin{aligned}\{Z_{2m-1}, Z_{2m}\} &= \{H^0_{2m-1}(\Psi; N), H^0_{2m}(\Psi; N)\} \\ &= (-1)^m 2\beta\{[\sin^2(\Psi_1) - \Psi_2^2 \cos(\Psi_1)], 0\}.\end{aligned} \tag{13}$$

It gives the state of the mth rod oscillator in terms of the state of the pendulum. Now geometry is introduced to draw a compact, global picture of the dynamics of the system at $\mu = 0$. In particular, the graph of the function $\mathbf{H}^0$, that is, all points in phase space satisfying

$$\mathscr{W}_0 = \{(\Psi, Z): Z = \mathbf{H}^0(\Psi; N)\}, \tag{14}$$

defines a two-dimensional vector–manifold (surface) parametrized by Ψ. This manifold is invariant since it is the geometric manifestation of the algebraic constraint (17) which upon differentiation with respect to time shows that $\dot{Z}$ is linearly related to $\dot{\Psi}$, that is, the vector field is tangent to the graph of $\mathbf{H}^0$. Now the dynamics residing on $\mathscr{W}_0$ are governed by a one-degree-of-freedom system, turning out to be, after substituting equation (12) into equation (10), the pendulum oscillator

$$\dot{\Psi}_1 = \Psi_2, \qquad \dot{\Psi}_2 = -\sin(\Psi_1). \tag{15}$$

Slow invariant manifold $\mathscr{W}_0$, an exact result, possesses the following properties:

$$\mathbf{H}^0(\hat{\Psi} = C; N) = \mathbf{H}^0(\hat{\Psi} = S_{\pm 1}; N) = 0, \tag{16a}$$

$$\frac{\partial \mathbf{H}^0}{\partial \Psi}(\hat{\Psi} = C; N) = \frac{\partial \mathbf{H}^0}{\partial \Psi}(\hat{\Psi} = S_{\pm 1}; N) = 0, \tag{16b}$$

$$\mathbf{H}^0(-\Psi; N) = \mathbf{H}^0(\Psi; N) = 0, \tag{16c}$$

$$\mathbf{H}^0(\Psi_1 + 2\pi, \Psi_2; N) = \mathbf{H}^0(\Psi_1, \Psi_2; N) = 0. \tag{16d}$$

Properties (16a) and (16b) render the manifold global since not only does it pass through all equilibria but also is tangent to the slow manifolds of the linearized

system about the equilibria. The slow invariant manifolds of the linearized system are nothing more than the familiar linear normal modes; they are spanned by the eigenvectors associated to the $O(1)$ eigenvalues. Linearization of the system about any of the equilibria reveals that its slow normal mode, a two-dimensional invariant manifold, coincides with the slow space Ψ. Property (16c) is a point reflective symmetry property; it along with periodicity property (16d) renders the dynamics on $\mathscr{W}_0$ identical to those of the uncoupled pendulum oscillator. It is seen that all properties (16) of the slow invariant manifold are present in the vector field of the uncoupled pendulum.

The focus here is on characterizing the purely slow dynamics of the coupled system. The global geometric picture of the purely slow dynamics at $\mu = 0$ naturally prompts the question whether the flexible rod/pendulum configuration admits slow dynamics governed by a one-degree-of-freedom system. Clearly this would be the case if the *global slow invariant manifold* $\mathscr{W}_0$ *is an approximation to a global slow invariant manifold for the coupled* ($\mu \neq 0$) *system*. We proceed to show that, under certain conditions, this is the case.

5. THE SLOW INVARIANT MANIFOLD

It is assumed that a slow invariant manifold exists in the phase space of the flexible rod/pendulum system. First, we will work on the slow dynamics of the finite system and then extend the results to the infinite system. By definition, for small coupling μ, an invariant manifold in phase space will be called slow if any motion initiated on it evolves on the slow time scale. It is assumed that such a manifold is two-dimensional and can be described by the graph of a vector-valued function $\mathbf{H}^\mu$ of the slow variable Ψ and the frequency ratio μ, i.e.,

$$\mathscr{W}^\mu = \{(Z, \Psi): Z = \mathbf{H}^\mu(\Psi; N)\}. \tag{17}$$

The union of the tangent planes at all points of the graph of the function $\mathbf{H}^\mu$ forms a smooth geometric object which is called the tangent vector bundle. The manifold $\mathscr{W}_\mu$ is invariant if and only if the vector field defined by the right hand side of equation (10) belongs to the tangent vector bundle of the graph of the function $\mathbf{H}^\mu$. The property of invariance is equivalent to the slow manifold condition,

$$\mathbf{B}(\Psi; N)\mathbf{H}^\mu(\Psi; N) + \mathbf{G}(\Psi; N) = \mu D_\Psi \mathbf{H}^\mu(\Psi; N)[\mathbf{F}(\Psi; N) + \mathbf{A}(\Psi; N)\mathbf{H}^\mu(\Psi; N)], \tag{18}$$

derived by first substituting equation (17) into equation (10b), and then using equation (10a). Partial differential equation (18) is solved approximately by representing its solution by the asymptotic series

$$\mathbf{H}^\mu(\Psi; N) = \mathbf{H}^0(\Psi; N) + \sum_{j=1}^{\infty} \mu^j \mathbf{H}^j(\Psi; N), \tag{19}$$

where

$$\mathbf{H}^j \equiv (\{H_1^j, H_2^j\}, \{H_3^j, H_4^j\}, \ldots, \{H_{2N-1}^j, H_{2N}^j\})^T.$$

Upon substituting series (19) into slow manifold condition (18), a recursive algorithm is obtained to determine the expansion terms. The computations are quite involved; they are carried out with the symbolic computer code MAPLE. Details are given in Appendix B.

It has been found that the approximation terms $\mathbf{H}^j$ in the series (19) depend explicitly on the order of truncation N through convergent sequencies of the frequency ratio μ_m. This is a pivotal result, since one can formally construct a slow manifold for the infinite system: It will be shown that the graph of the vector-valued function

$$\begin{aligned}\mathbf{H}^{\mu}(\Psi) &\equiv \lim_{N\to\infty} \mathbf{H}^{\mu}(\Psi; N)\\ &= \lim_{N\to\infty} (\{H_1^j(\Psi, N), H_2^j(\Psi, N)\}, \ldots, \{H_{2N-1}^j(\Psi, N), H_{2N}^j(\Psi, N)\})^T \end{aligned} \tag{20}$$

defines a slow manifold of the flexible rod/pendulum system, that is, for $N = \infty$. Physically, this would imply that the coupled system undergoes slow periodic motions close to those of the pendulum supported by a perfectly rigid rod.

The computations reveal that the pair elements of equation (20) depend explicitly on the frequency ratios μ_m. In particular, the mth pair element admits the compact expression

$$\{H_{2m-1}^{\mu}(\Psi; \mu_m), H_{2m}^{\mu}(\Psi; \mu_m)\} = (-1)^m 2\beta\{H_1^{\mu}(\Psi; \mu_m), H_2^{\mu}(\Psi; \mu_m)\}. \tag{21}$$

The computations reveal that the dependence of the pair (21) on the frequency ratios is of $O(\mu^2\mu_m^2)$ and $O(\mu^3\mu_m)$. Therefore, the factor enclosed by brackets on the left hand side of equation (21) converges as $\mu_m \to 0$, equivalently as $m \to \infty$, i.e.,

$$\{H_1^{\mu}(\Psi), H_2^{\mu}(\Psi)\} \equiv \lim_{\mu_m\to 0} \{H_1^{\mu}(\Psi; \mu_m), H_2^{\mu}(\Psi; \mu_m)\}. \tag{22}$$

The graph of equation (22) defines an envelop manifold for the manifolds defined by the pair-elements of equation (20). We have computed the approximation

$$\{H_1^{\mu}(\Psi), H_2^{\mu}(\Psi)\} = (-1)^m 2\beta[\{\hat{H}_1^{\mu}(\Psi), \hat{H}_2^{\mu}(\Psi)\} + O(\mu^4)], \tag{23}$$

where

$$\hat{H}_1^{\mu}(\Psi) = +\mu^2 2\beta\sigma_1\{7\Psi_2^2 \cos^2(\Psi_1) + [4 - \Psi_2^4]\cos^3(\Psi_1) - 11\Psi_2^2 \cos^4(\Psi_1)\}, \tag{24a}$$

$$\begin{aligned}\hat{H}_1^{\mu}(\Psi) &= 2\beta[\sin^2(\Psi_1) - \Psi_2^2 \cos(\Psi_1)]\\ &\quad + \mu^2 2\beta\sigma_1\{7\Psi_2^2 \cos^2(\Psi_1) + [4 - \Psi_2^4]\cos^3(\Psi_1) - 11\Psi_2^2 \cos^4(\Psi_1)\}, \end{aligned} \tag{24a}$$

$$\begin{aligned}\hat{H}_2^{\mu}(\Psi) &= \mu 2\beta \sin(\Psi_1)\Psi_2\{[\Psi_2^2 + 4\cos(\Psi_1)]\\ &\quad + \mu^2\sigma_1\{[-34 + 5\Psi_2^4]\cos^2(\Psi_1) + 75\Psi_2^2 \cos^3(\Psi_1) + 50\cos^4(\Psi_1)\}\}. \end{aligned} \tag{24b}$$

The envelop slow manifold, which is described by the graph of the pair (22), suffices to characterize the slow motions of the rod. In fact, the state of the mth rod oscillator is given by

$$\{H^{\mu}_{2m-1}(\Psi;\mu_m), H^{\mu}_{2m}(\Psi;\mu_m)\} = (-1)^m 2\beta[\{H^{\mu}_1(\Psi), H^{\mu}_2(\Psi)\} + O(\mu^2\mu_m^2) + O(\mu^3\mu_m)]. \tag{25}$$

Therefore, the vector-valued function $\mathbf{H}^{\mu}(\Psi)$ is well defined since it is an infinite sequence converging to a finite limit. It defines a two-dimensional vector-valued manifold in the phase space setting of the infinite system. The slow manifold satisfies the properties (16) of the zeroth order slow invariant manifold. Thus, there is hope that the slow manifold computed is an approximation to an invariant.

The amplitude of a motion on the slow manifold is a smooth function of the energy level since the manifold is a smooth function of Ψ. Let ω_p and ω_r denote the fundamental frequencies of the pendulum and rod for a motion on the slow manifold. From equation (24) it is concluded that $\omega_r = 2\omega_p$ if the motion has energy less than the energy of the saddle-center, that is, the pendulum *librates* and that $\omega_r = \omega_p$ if the motion has energy greater than the energy of the saddle-center, that is, the pendulum *whirls*. Regarding the rod modal oscillators, from equation (25) it can be seen that the *odd ones are out-of-phase with the even ones*. The conclusion is that all rod modal oscillators do behave qualitatively the same.

5.1. THE SLOW REDUCED DYNAMICS

The existence of an invariant manifold introduces the notion of dimension reduction. The restriction of the dynamics of the infinite-dimensional system to the slow invariant manifold are described by the slow non-linear oscillator defined by

$$\dot{\Psi} = N_{\mu}(\Psi) \equiv \lim_{N\to\infty} [\mathbf{F}(\Psi; N) + \mathbf{A}(\Psi; N)\mathbf{H}^{\mu}(\Psi; N)] \tag{26}$$

along with $Z = \mathbf{H}^{\mu}(\Psi)$. Upon using the analytic expression for the slow manifold, oscillator (26) takes the first-order form

$$\dot{\Psi}_1 = \Psi_2, \qquad \dot{\Psi}_2 = -\left[1 + 2\beta\pi^2 \sum_{j=1}^{\infty} \mu^{2j} F_{2j}(\Psi_1, \Psi_2)\right] \sin(\Psi_1). \tag{27}$$

The equilibrium points of this oscillator are identical to those of the uncoupled pendulum oscillator. The perturbation terms F_{2j} satisfy the properties

$$F_{2j}(-\Psi_1, -\Psi_2) = -F_{2j}(\Psi_1, \Psi_2), \qquad F_{2j}(\Psi_1 + 2\pi, \Psi_2) = F_{2j}(\Psi_1, \Psi_2). \tag{28a, b}$$

Because of the above symmetry and periodicity properties, the phase portrait of oscillator (27) is topologically equivalent to that of the uncoupled pendulum, for sufficiently small (weak) coupling μ. Note that it is precisely the global properties of the slow manifold that endow the slow oscillator with the global properties of the uncoupled pendulum.

Upon using the $O(\mu^2)$ approximation to the slow manifold, we obtain the corresponding approximation to the slow oscillator (26) whose second-order form is

$$\ddot{\theta} + [1 + P_\mu(\theta, \dot{\theta})\dot{\theta}^2 + Q_\mu(\theta)] \sin(\theta) = 0, \tag{29}$$

where

$$4P_\mu(\theta, \dot{\theta}) \equiv \mu^2\beta\pi^2[7 - 11\cos^2(\theta) - \dot{\theta}^2\cos(\theta)],$$
$$Q_\mu(\theta) \equiv \mu^2\beta\pi^2[\cos(\theta) - \cos^3(\theta)].$$

It can be shown that the quantities

$$M_\mu(\theta, \dot{\theta}) \equiv \exp\left(\int_0^\theta P_\mu(\eta, \dot{\eta})\, d\eta\right), \qquad T_\mu(\theta, \dot{\theta}) \equiv \tfrac{1}{2}M_\mu(\theta, \dot{\theta})\dot{\theta}^2, \tag{30a, b}$$

$$V_\mu(\theta, \dot{\theta}) \equiv \int_0^\theta M_\mu(\eta, \dot{\eta})[1 + Q_\mu(\eta)]\, d\eta \tag{30c}$$

play, respectively, the roles of mass, kinetic and potential energies. In fact, it can be shown that the energy is given by

$$E_\mu = T_\mu + V_\mu = E_0 + O(\mu^2), \tag{31}$$

where E_0 is the total energy of the uncoupled pendulum. The conclusion is that the flexible rod/pendulum dynamical system has been reduced to a *one-degree-of-freedom system*, *which turns out to be a regular conservative perturbation of the uncoupled soft substructure*, *that is*, *the pendulum*.

Clearly, if a slow invariant manifold exists and possesses global properties (16), then it carries a slow motion connecting the saddle-centers, that is, a heteroclinic motion. Since the dynamics restricted to the slow manifold are described by an oscillator, which is a regular perturbation of the uncoupled pendulum, one can apply the Melnikov technique [3] to show the existence of the heteroclinic motion. The challenging problem is not to assume *a priori* knowledge of a slow invariant manifold and try to modify the Melnikov technique for a singular rather than a regular perturbation of the uncoupled pendulum. Recall that the flexible rod/pendulum system is considered as a singular perturbation of the uncoupled pendulum. In contrast to a regular perturbation where the dimension of the dynamics remains constant, a singular perturbation results in increase of dimension. Nevertheless, the analysis suggests through the analytic computation of the slow manifold the existence of a heteroclinic motion for weak (sufficiently small) coupling μ.

5.2. THE SLOW PHASE PORTRAIT

Up to this point, formal analytic approximation to a slow manifold have been constructed and the oscillator describing the dynamics restricted to it has been computed. To the best of our knowledge there is no theorem to guarantee the existence of global two-dimensional invariant manifold for our infinite

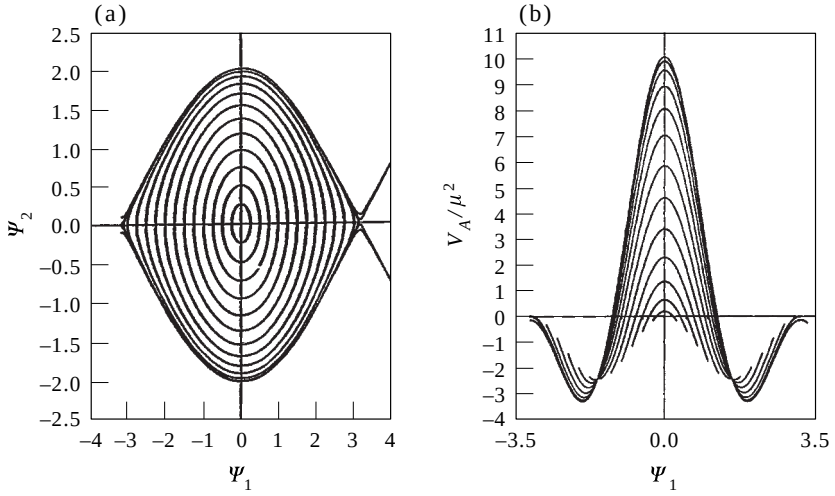

Figure 2. Projections of a set of motions initiated on the computed slow manifold: (a) onto the pendulum phas plane, (b) onto the configuration plane at the rod end A. System parameters: $\mu = 0{\cdot}025$, $\beta = 1{\cdot}0$, $N = 32$.

dimensional conservative system. A smooth two-dimensional invariant manifold of a conservative dynamical system is composed necessarily of a family of periodic motions whose amplitude or norm varies continuously with the energy level. The members of the family must share common properties. One way to verify the existence of a smooth invariant manifold is to systematically generate numerically a family of periodic motions sharing common properties and being continuous with respect to the energy level.

The analytic results will be used to perform numerical experiments to verify the fact that indeed the slow manifold that has been computed approximates an invariant manifold. A set of motions are initiated on the $O(\mu^4)$ slow manifold. This order of approximation is readily computed from the analytic computations in Appendix B. The energy level is varied from that of the center C to above that of the saddle-center $S_{\pm 1}$. Figure 2(a) shows the projection of this set of motions onto the phase plane of the pendulum, whereas Figure 2(b) shows its projection onto the configuration plane $\Psi_1 - V_A/\mu^2$. Clearly the portrait shown in Figure 2(a) resembles that of the uncoupled pendulum. We claim that this is the phase portrait of the *exact* slow oscillator (26). Figure 2(b) shows that the motions trace open curves, a feature reflecting the fact that the motions are periodic. Thus, all motions initiated on the slow manifold are periodic and depend continuously on the energy level. Thus, the totality of the slow periodic motions forms a slow invariant manifold. They have symmetry properties identical to those predicted by the analytic approximations to the slow manifold. Thus, the computed slow manifold is indeed in the neighborhood of an *invariant* slow manifold.

6. THE NATURE OF THE SLOW NORMAL MODE

It is common practice in engineering to study structural and mechanical dynamical systems in the context of normal modes [14–16]. The two-dimensional

slow invariant manifold can be identified with a non-linear normal mode since all motions residing on it share common properties that can be used to define vibrations-in-unison [14]. Figure 2(b) reveals the following common properties: (1) the motions are periodic and their energy level varies continuously; (2) whenever the pendulum mass swings through its zero position the flexible rod reaches its maximum displacement; (3) whenever the pendulum reaches its maximum displacement, the rod velocity vanishes; (4) whenever the rod displacement becomes zero, the pendulum displacement is not zero. The above properties are used to define a family of vibrations-in-unison. For the particular problem, because of the global non-linear character of the invariant manifold, the properties of the motions on the manifold are not identical to the classical definition of vibrations in-unison [14]. The classical definition [14, 15, p. 2] requires that during a normal mode *the pendulum and rod displacements reach their maximum and maximum values at the same time instant*. Here this property is not satisfied. The new property is *whenever the pendulum crosses zero the rod attains its maximum displacement*. This property is qualitatively different than the above classical property. Nevertheless, the common properties define a distinct mode of motion and thus we identify the global non-linear slow invariant manifold with a global *nonlinear slow normal mode* of oscillation. In reference [16] a local two-dimensional invariant manifold passing through a stable equilibrium is identified with a local normal mode. Here it is shown that a global two-dimensional invariant manifold, in an infinite-dimensional phase space, carrying a multitude of stable and unstable equilibrium states is the geometric realization of a global normal mode of motion.

Now the geometric realization of the slow normal mode as a two-dimensional manifold parametrized by the state of the pendulum separates the dynamics on the manifold into the master dynamics, associated with the soft substructure (pendulum), and the slaved dynamics, associated with the stiff substructure (rod). Physically, the stiff substructure is driven by the slow motions of the soft substructure. For a generic purely slow motion, the position and velocity fields of the stiff flexible rod are given by

$$V(\xi, \tau) = \mathscr{H}_1^{\mu}(\xi, \theta(\tau), \dot{\theta}(\tau)) \equiv \mu^2 \sum_{m=1}^{\infty} \mu_m^2 H_{2m-1}^{\mu}(\theta(\tau), \dot{\theta}(\tau); \mu_m)\phi_m(\xi), \quad (32a)$$

$$\dot{V}(\xi, \tau) = \mathscr{H}_2^{\mu}(\xi, \theta(\tau), \dot{\theta}(\tau)) \equiv \mu \sum_{m=1}^{\infty} \mu_m^2 H_{2m}^{\mu}(\theta(\tau), \dot{\theta}(\tau); \mu_m)\phi_m(\xi). \quad (32b)$$

The contribution of the rod modal oscillators to the rod displacement is hierarchical. In particular, the rod modal oscillators close to the pendulum contribute the most to the slaved slow motion of the rod. The contribution decays as fast as $\mu_m^2 \equiv 1/(2m-1)^2$: the faster the time scale the smaller the contribution. Thus, for a sufficiently stiff flexible rod, the dynamics of the flexible rod/pendulum system can be approximated by a two-degree-of-freedom system consisting of a stiff linear oscillator coupled to a pendulum oscillator [12].

The slow dynamics of the stiff rod is part of a normal mode. Thus, they should be factored out into a time component and a space component. Upon using the analytic expression for the slow manifold (23), one obtains

$$\mathscr{H}_1^{\mu}(\xi, \theta(\tau), \dot{\theta}(\tau)) = [2\beta\mu^2 \hat{H}_1^{\mu}(\theta(\tau), \dot{\theta}(\tau)) + O(\mu^6)]\hat{\Phi}(\xi), \tag{33a}$$

$$\hat{\Phi}(\xi) \equiv \sum_{m=1}^{\infty} (-1)^m \mu_m^2 \phi_m(\xi), \tag{33b}$$

where the function $\hat{\Phi}(\xi)$ is the spatial distribution of the slaved component of the slow normal mode. During a slow motion all rod modal oscillators, equivalently all spatial points, attain their extrema simultaneously at equi-periodic time instances. This is how spatio-temporal coherence manifests itself. Let $A_{2m-1} \equiv Z_{2m-1}$ whenever the velocity of the first rod oscillator is zero. Then the shape of the rod during a slow motion is given by

$$\Phi_s(\xi) \equiv \sum_{m=1}^{\infty} A_{2m-1} \mu_m^2 \phi_m(\xi). \tag{34}$$

Figure 3(a) plots the rod displacement for a slow motion versus the rod displacement predicted by equation (33a). The slope is almost unity. Thus, the slow motion of the rod is predicted exceptionally well by equation (33a). Figure 3(b) shows that the shape the rod attains when its momentum is zero is approximated exceptionally well by the function (33b). Notice that the slope of the mode at $\xi = 1$ is not zero. This is in agreement with the non-zero natural boundary conditions at the end A of the rod.

On the other hand, the master slow dynamics are described by the oscillator

$$\ddot{\theta} + [1 - \ddot{\mathscr{H}}_1^{\mu}(\xi = 1, \tau)] \sin(\theta) = 0, \tag{35}$$

where $\ddot{\mathscr{H}}_1^{\mu}(\xi = 1, \tau)$ denotes the acceleration of the rod end A, where the pendulum is attached, for a slow motion.

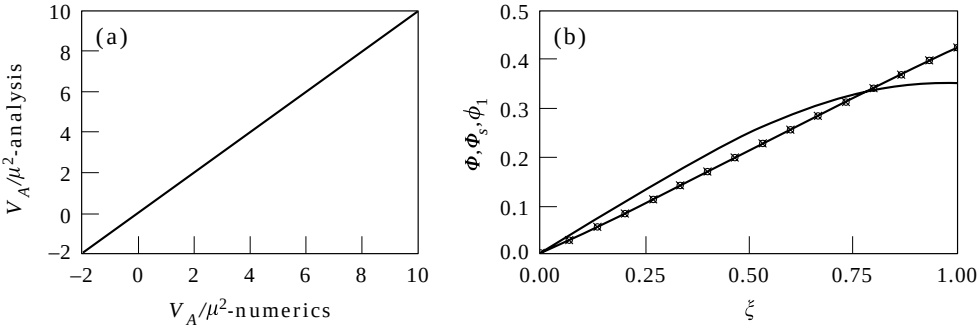

Figure 3. Prediction of the spatio-temporal characteristics of the slow motions of the flexible rod: (a) amplitude of the rod end A, (b) spatial shape of the slow mode. System parameters: $\mu = 0{\cdot}025$, $\beta = 1{\cdot}0$, $N = 32$. ——, First linear mode; ○, GSP theory; ×, section of zero momentum.

Upon using the expression for the slow invariant manifold, one has the approximation

$$\ddot{\mathscr{H}}_1^{\mu}(\xi = 1, \tau) = \mu\sigma_4 \left[\frac{\partial H_2^{\mu}(\theta(\tau), \dot{\theta}(\tau))}{\partial \theta(\tau)} \theta(\tau) + \frac{\partial H_2^{\mu}(\theta(\tau), \dot{\theta}(\tau))}{\partial \dot{\theta}(\tau)} \ddot{\theta}(\tau) \right]$$

$$+ O(\mu^3 \mu_m^2) + O(\mu^4 \mu_m),$$

$$\sigma_4 \equiv \sum_{m=1}^{\infty} (-1)^{m+1} \mu_m^2. \tag{36}$$

In view of equation (36), the slow oscillator (35) takes the form

$$M_{\mu}(\theta, \dot{\theta})\ddot{\theta} + K_{\mu}(\theta, \dot{\theta}) \sin(\theta) = 0, \tag{37}$$

with mass and stiffness defined by

$$M_{\mu}(\theta, \dot{\theta}) \equiv 1 - \mu\sigma_4 \frac{\partial H_2^{\mu}(\theta, \dot{\theta})}{\partial \dot{\theta}} \sin(\theta), \tag{38a}$$

$$K_{\mu}(\theta, \dot{\theta}) \equiv 1 - \mu\sigma_4 \frac{\partial H_2^{\mu}(\theta, \dot{\theta})}{\partial \theta} \dot{\theta}. \tag{38b}$$

In section 5.1 it was shown that, for weak coupling, the dynamics of the slow oscillator are qualitatively the same as those of the uncoupled pendulum. However, since the mass and stiffness of the slow oscillator depend on the geometry of the slow invariant manifold, qualitative changes in the dynamics are possible at points in phase space where the manifold bifurcates or folds. At such points, which signal critical energy levels, the frequency of the slow oscillator vanishes. This clearly happens, numerical experiments reveal it, whenever $\partial H_2^{\mu}(\theta, \dot{\theta})/\partial \dot{\theta} \to \infty$. The series expansion fails to capture these bifurcations. However, it approximates the slow invariant manifold, the fundamental geometric object from which such qualitative changes could emanate.

7. STABILITY OF THE SLOW NORMAL MODE

In this section, the orbital stability of the slow invariant manifold is studied. The slow manifold is orbitally stable if all motions residing on it are orbitally stable with respect to transversal perturbations [11]. To address qualitatively the issue of stability, the transformation $Z = \mathbf{H}_{\mu}(\Psi) + Y$ and slow manifold condition (18) are used to express the original system (10) as

$$\dot{\Psi} = \mathbf{N}_{\mu}(\Psi) + \mathbf{A}(\Psi)Y, \qquad \mu\dot{Y} = \mathbf{B}(\Psi)Y. \tag{39a, b}$$

The variable Y measures the transverse distance of a motion from the slow manifold. If $Y = 0$, the above equation reduces to the exact oscillator (26) describing the dynamics on the slow manifold. Equation (39b) reveals that the dynamics in the neighborhood of the slow manifold are described by linear oscillators parametrically forced by the slow motions on the invariant manifold.

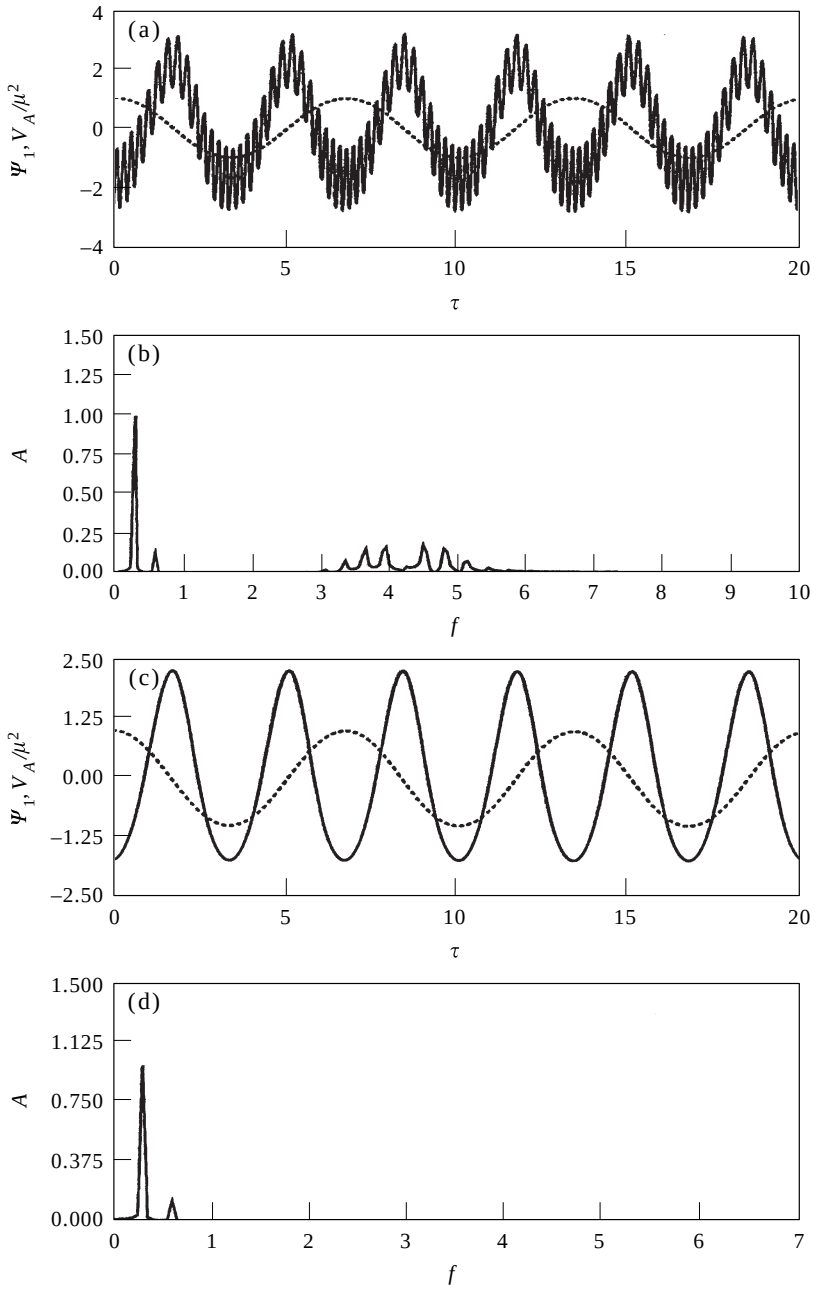

Figure 4. Time histories and frequency spectra of the pendulum and rod displacements: (a) motion initiated off the slow manifold, (b) spectrum of rod displacement, (c) motion initiated on the $O(\mu^4)$ approximation to the slow manifold, (d) spectrum of rod displacement. System parameters: $\mu = 0{\cdot}025$, $\beta = 1{\cdot}0$, $N = 32$. ——, Flexible rod; – – –, pendulum.

Figure 4(a) shows that a motion initiated close to the slow manifold evolves on slow and fast time scales. Figure 4(b) reveals a gap in the frequency spectrum of the rod motion. The spectrum gap separates a group of low frequencies that are

multiples of the pendulum frequency from a group of high frequencies with upper bound slightly below the fundamental frequency $1/\mu$ of the uncoupled rod. The group of high frequencies is due to the non-linear coupling between the slow manifold and the transversal fast dynamics; see equation (39a). Numerical experiments reveal that the amplitudes of the high oscillations decrease as the transverse distance of the initial conditions from the slow manifold decreases, that is, as $\| Y(0)\| \to 0$. This reflects the orbital stability of the slow manifold. Figures 4(c, d) show the absence of high oscillations if the motion is initiated on the slow invariant manifold.

7.1. LYAPUNOV CHARACTERISTIC EXPONENTS

The slow dynamics are prone to transverse instabilities since the fast dynamics are parametrically excited by the slow invariant manifold. To address the issue of orbital stability, the Lyaponov characteristic exponents of motions on the slow manifold and motions in its neighborhood are computed. The system is considered at $N = 1$, which is an oscillator/pendulum system with equations of motion:

$$\dot{\Psi}_1 = \Psi_2, \qquad I_1(\Psi_1)\dot{\Psi}_2 = -[1 + 2\beta(1 - \Psi_2^2 \cos(\Psi_1)) + Z_1] \sin(\Psi_1),$$
$$\mu\dot{Z}_1 = Z_2, \qquad \mu I_1(\Psi_1)\dot{Z}_2 = -Z_1 + 2\beta[\Psi_2^2 \cos(\Psi_1) - \sin^2(\Psi_1)], \tag{40}$$

where $I_1(\Psi_1) \equiv 1 + 2\beta \cos^2(\Psi_1) \neq 0$. Recall that, for weak coupling, all rod modal oscillators behave identically. Thus, truncation at $N = 1$ is justified. Let $P(0)$ be a point in the four-dimensional phase space of equations (40) and $\hat{\mathbf{n}}$ be a unit vector attached to it. The average exponential divergence of the trajectory passing through $P(0)$ in the direction $\hat{\mathbf{n}}(0)$ is measured by the quantity

$$\lambda(P(0), \hat{\mathbf{n}}(0)) \equiv \lim_{\tau \to \infty} \frac{1}{\tau} \ln \|\mathbf{n}(\tau)\|, \tag{41}$$

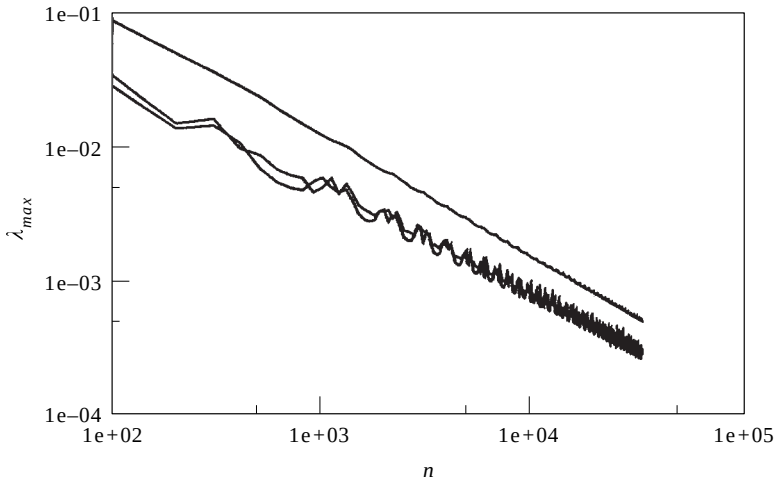

Figure 5. Behavior of the maximum Lyaponov characteristic exponent for motions initiated on and off the slow manifold. System parameters: $\mu = 0{\cdot}025$, $\beta = 1{\cdot}0$, $N = 1$.

where $\hat{\mathbf{n}}(\tau)$ is the solution, initiated at $\mathbf{n}(0)$, of the linearization of equations (40) about the motion passing through $P(0)$. The linearized system is given by

$$\dot{\eta}_1 = \eta_2, \qquad I_1(\Psi_1)\dot{\eta}_2 = J_{21}(\Psi, Z_1)\eta_1 + J_{22}(\Psi)\eta_2 + J_{23}(\Psi)\zeta_1,$$
$$\mu\dot{\zeta}_1 = \zeta_2, \qquad \mu I_1(\Psi_1)\dot{\zeta}_2 = J_{41}(\Psi, Z_1)\eta_1 + J_{42}(\Psi)\eta_2 + J_{43}(\Psi)\zeta_1. \tag{42}$$

The various coefficients are given in Appendix C. The number $\lambda(P(0), \hat{\mathbf{n}}(0))$ is the so-called Lyapunov characteristic exponent (LCE). A genetic motion is characterized by four LCEs measuring exponential divergence along the elements of the natural basis $\{\hat{\mathbf{e}}_j\}_{j=1}^{j=4}$.

Using the procedure in reference [4], all four LCEs have been computed. Figure 5 shows how the maximum Lyapunov exponent λ_{max} behaves as the number of iterates increases. It apparently converges to zero. This is the typical behavior of exponents for a region of phase space that is ordered [4], that is, filled with periodic and quasi-periodic motions. For sufficiently small μ, one finds that all motions initiated on the slow invariant manifold and near it have zero Lyapunov exponents. Based on extensive numerical experiments, it is concluded that indeed the slow invariant manifold is orbitally stable.

The slow invariant manifold is an equilibrium for the transversal fast motions. There can be at least two types of interaction between the slow and fast dynamics. Suppose the manifold is stable, then the slow dynamics interact with the fast dynamics due to the non-linear coupling to expand the spectrum of the high frequencies, as shown in Figure 4(b). The second interaction is due to loss of stability of the slow manifold and geometric changes such as folding. Interaction is expected to occur at the energy level of the saddle-centers $S_{\pm 1}$ at some critical coupling μ_{cr}. This is so since according to KAM theory (4) their one-dimensional invariant manifolds could intersect transversely to cause motions sensitive in initial conditions, that is, chaotic (stochastic according to reference [4]) motions.

8. THE HETEROCLINIC MOTION AND STOCHASTICITY

Recall that at $\mu = 0$ the system coincides with the uncoupled pendulum which possesses a heteroclinic motion. Hyperbolic structures such as homoclinic and heteroclinic motions can cause complex dynamics such as stochastic motions in conservative systems. The question is whether the *heteroclinic motion will be perturbed to a heteroclinic one for the coupled* ($\mu \neq 0$) *system*. On one hand, it is well known that the heteroclinic motion of the pendulum oscillator and the homoclinic motion of the Duffing oscillator can be destroyed if these oscillators are perturbed by rapidly varying external forces. The splitting of the invariant manifolds that make the heteroclinic motion is exponentially small [17, 18]. It is conjectured that chaos will be undetected in numerical experiments. On the other hand, the present analysis, for sufficiently small coupling μ, suggests that the one-dimensional stable and unstable invariant manifolds of the saddle-centers should coincide to form a heteroclinic motion residing on the slow invariant manifold. We conjecture that, since on the slow manifold the rod is driven by the pendulum, the heteroclinic motion cannot be destroyed by the fast oscillations

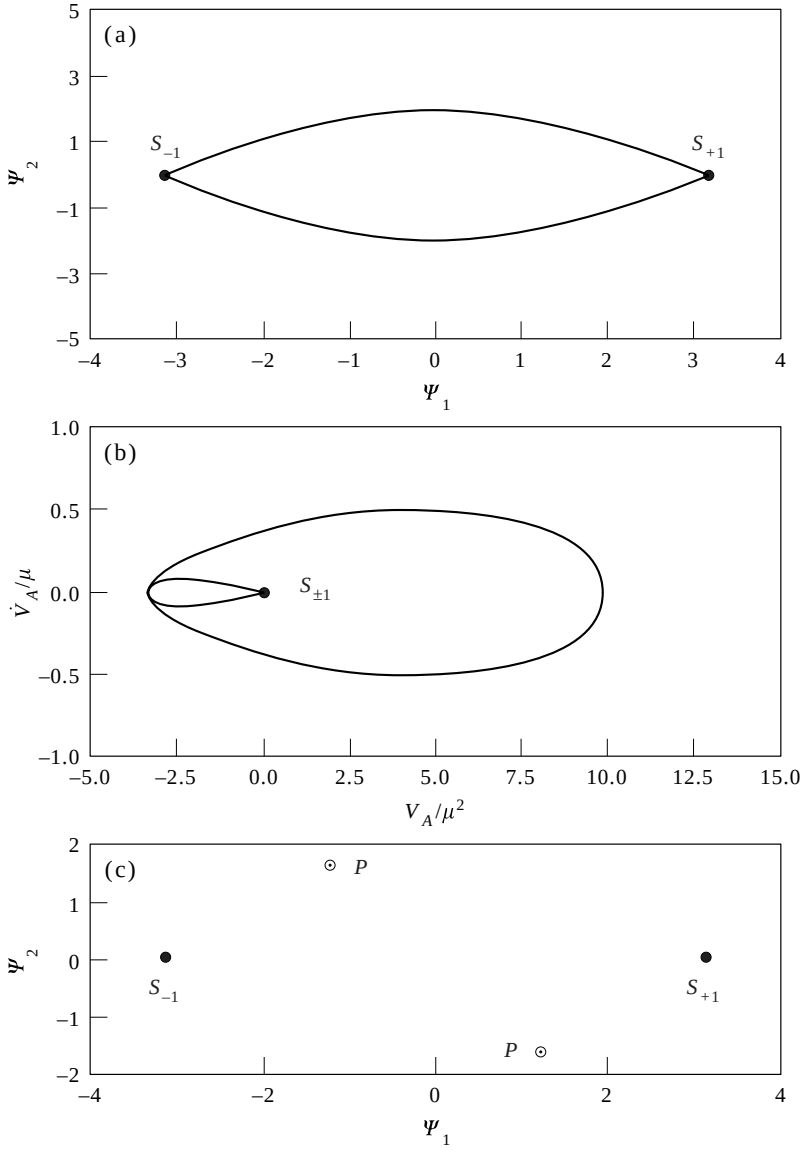

Figure 6. Projections of a near heteroclinic motion onto: (a) the pendulum phase plane, (b) the phase plane of the rod end A, (c) Poincare map. System parameters: $\mu = 0{\cdot}0250$, $\beta = 1$, $N = 32$.

generated by the stiff rod. In this section, several numerical experiments are performed to study the nature of motions initiated on the unstable one-dimensional invariant manifold of the saddle-center S_{+1}. Such a motion will be referred to as a *near heteroclinic* (NH) motion. The experiment aims at verifying the fact that the coupled system possesses a heteroclinic motion, and showing that the slow manifold (the slow normal mode) creates stochastic motions at the energy level of the unstable equilibrium above some critical coupling.

For coupling $\mu = 0{\cdot}025$ and mass ratio $\beta = 1$, Figures 6(a) and (b) show the projection of a NH motion onto the pendulum phase plane and the rod phase

plane at the end A. Note that the near singular points of the projected trajectories are near the corresponding projections of the saddle-centers $S_{\pm 1}$. The trajectory in the pendulum phase space resembles that traced by the heteroclinic motion of the uncoupled pendulum. Figure 6(c) shows that the Poincare map of this motion, created by the section $Z_1 = 0$, $Z_2 > 0$, consists of almost four distinct points. The double point P is the signature of a periodic motion on the slow manifold. Recall that for a motion on the slow manifold the frequency of the rod is twice that of the pendulum. However, Figure 7(a) zooms in at point S_{+1} to reveal a very thin layer of stochasticity. The one mode approximation behaves the same. It is used to compute the Lyapunov characteristic exponents of the NH motion. Figure 7(b) shows that this motion has a maximum Lyapunov exponent $\lambda_{max} \approx 5 \times 10^{-5}$. During the simulation, the energy level was kept constant to the ninth digit. The integration routine uses an adaptive time step. Figure 7(c) shows the FFT of the stochastic motion. Here only low frequencies are seen since the high frequency ($f = 6{\cdot}3662$ Hz) is absent from the spectrum. Figure 7(d) shows the spectrum of a motion whose energy level is slightly smaller than that of the stochastic motion. The motion is periodic and clearly has frequency distribution similar to that of the NH motion save the fact that the latter has a near continuous spectrum.

The coupling strength is increased and how the shape of stochasticity changes is explored. Over the range $\mu \in [0{\cdot}025, 0{\cdot}050]$ its length and thickness increase. It

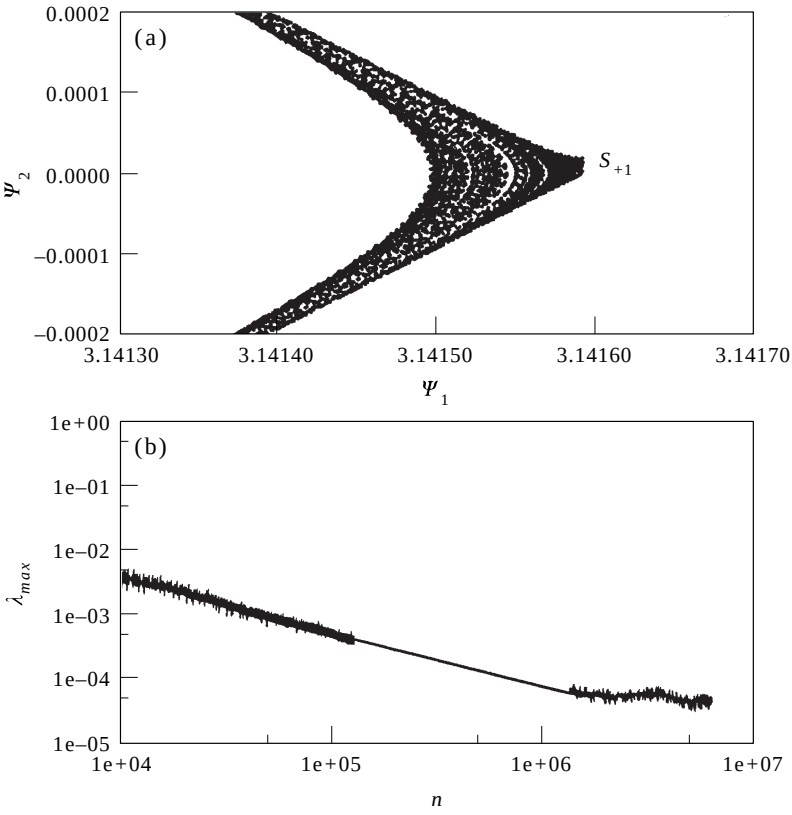

Figure 7. *Caption overleaf*.

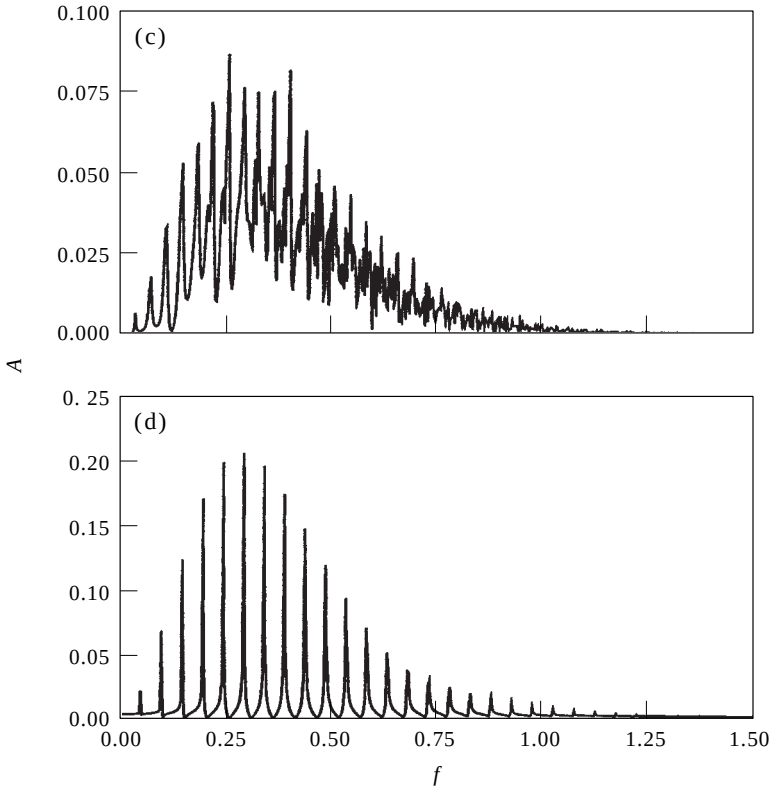

Figure 7. (a) Detail of the Poincare map around point S_{+1}, (b) maximum Lyapunov characteristic exponent (6 450 300 iterates), (c) frequency spectrum, (d) frequency spectrum of a motion with energy level slightly less than that in (c). System parameters: $\mu = 0{\cdot}0250$, $\beta = 1$, $N = 32$.

consists of two almost symmetric pieces; see Figure 8(a). Over the range $\mu \in [0{\cdot}050, 0{\cdot}075]$ the thickness of the stochasticity layer grows unevenly while its two pieces approach each other (see Figure 8(b)) to eventually be connected (as shown in Figure 8(c)) to form a cloud that continues to diffuse into even larger regions of the phase space as the coupling is further increased. The spread of stochasticity is reminiscent of the so-called Arnold diffusion in the KAM theory, addressing stochasticity in Hamiltonian conservative systems [4].

The qualitative changes of the Poincare map are reflected in the frequency spectrum. Figure 9(a) shows the frequency spectrum of the displacement of the rod end A for the NH motions whose Poincare maps are shown in Figure 8(a). Clearly, when the layer of stochasticity consists of two pieces of uniform thickness, the spectrum is segmented into a group of low frequencies and a group of high frequencies. If the value of coupling is decreased, the spectral gap becomes wider. It seems that at some value of coupling the fast frequencies disappear. If the value of coupling is increased, the spectral gap narrows to cause collision of slow and fast frequencies and subsequent intermixing of the two pieces of the stochasticity layer. This seems to cause a strong interaction between the slow and fast time scales. This is seen in Figures 9(b) and (c), corresponding to Figures 8(b) and (c).

To quantify the strength of stochasticity, the Lyapunov exponents for the $N = 1$ system, that is, the oscillator/pendulum have been computed. Figure 10 shows in a logarithmic scale the behavior of the maximum Lyapunov characteristic exponent λ_{max} as a function of iterations for $\mu = 0{\cdot}025, 0{\cdot}050, 0{\cdot}075, 0{\cdot}10$. Clearly, it can be seen that there exists a critical μ_{cr} above which there is apparent convergence to a positive number and below it there is apparent convergence to a small positive value. Here it can be seen that there is a large change in the value of the maximum LCEs as the coupling crosses the critical value of coupling. It seems that the change has to do with the interaction between the slow and fast dynamics. Recall that for small coupling stochastic motions were found evolving on the slow time scale.

Next the value of coupling is decreased to $\mu = 0{\cdot}001$. For a near heteroclinic motion, Figures 11(a) and (b) show respectively the frequency spectrum of the rod

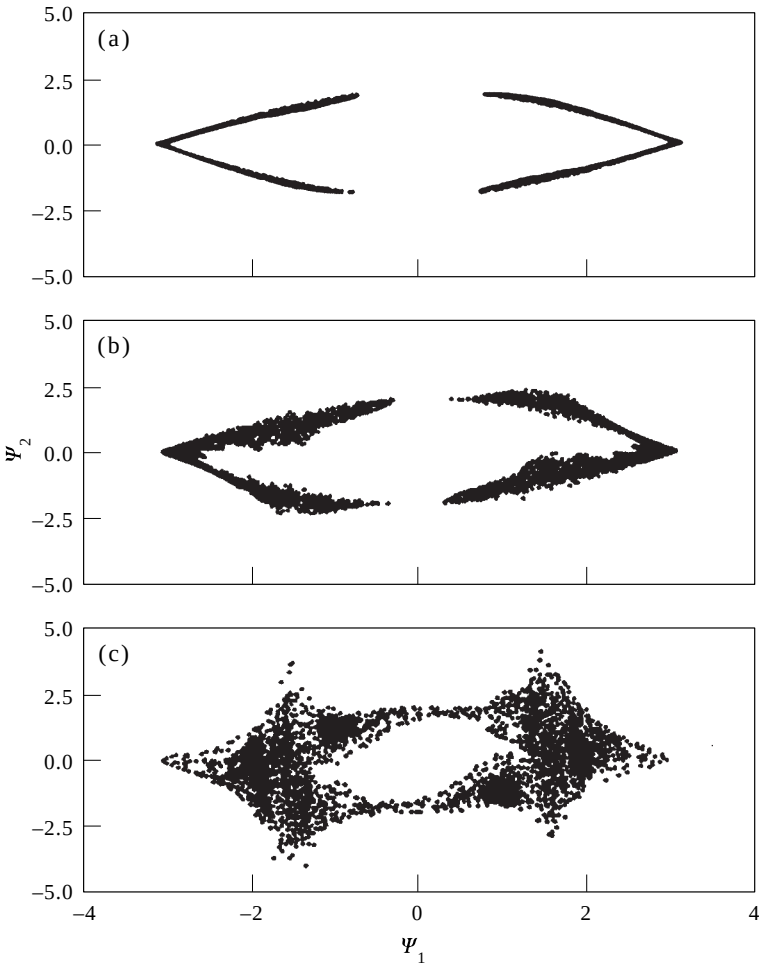

Figure 8. Evolution of Poincare map of near heteroclinic motions: (a) $\mu = 0{\cdot}050$, (b) $\mu = 0{\cdot}075$, (c) $\mu = 0{\cdot}100$. System parameters: $\beta = 1$, $N = 32$.

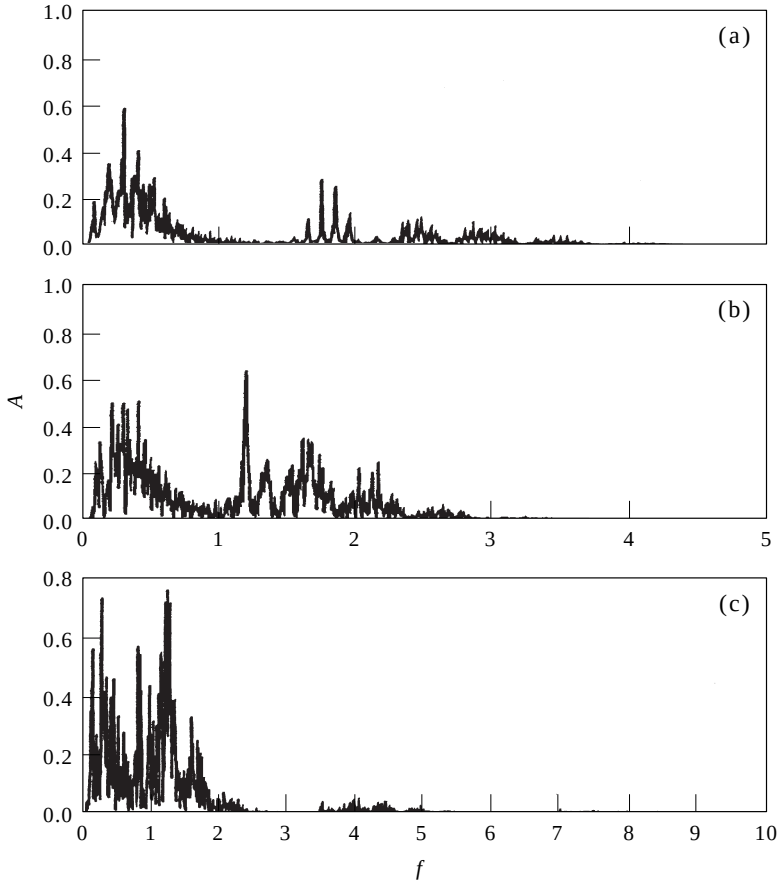

Figure 9. Fast Fourier Transforms of near heteroclinic motions: (a) $\mu = 0{\cdot}050$, (b) $\mu = 0{\cdot}075$, (c) $\mu = 0{\cdot}100$. System parameters: $\beta = 1$, $N = 32$.

and the pendulum. Figure 11(c) shows that the two positive Lyapunov exponents converge to zero. The existence of a heteroclinic motion has thus been verified.

9. DISCUSSION

This work presents the global geometric structure of the slow dynamics of a coupled system that consists of a stiff linear elastic rod coupled to a pendulum. The slow dynamics form a family, parametrized by the energy level, of periodic motions including a heteroclinic one. In phase space, this family of slow motions forms a non-linear two-dimensional invariant manifold. This manifold is the geometric manifestation of a non-linear normal mode of motion. By transforming the equations of motion into a singular perturbation problem, this manifold was computed, and thus the family of slow periodic motions was determined. Upon establishing the existence of the slow invariant manifold, one has the interesting result that the coupled system undergoes periodic motions during which the pendulum substructure slaves the rod substructure into slow periodic motions. This result is important since if dissipation is added, the slow invariant manifold

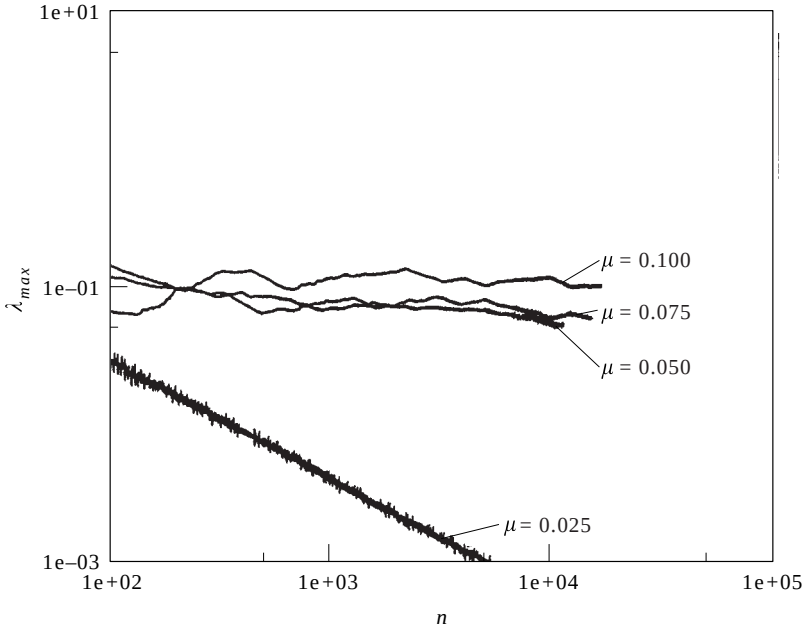

Figure 10. Behavior of the maximum Lyapunov characteristic exponent with the coupling μ for the near heteroclinic motions. System parameters: $\beta = 1$, $N = 1$.

becomes an attractive invariant manifold for the dissipative system [19]. This means that the dynamics after some initial time phase are slow and thus dominated by the dynamics of the pendulum substructure since the slaved dynamics of the stiff rod substructure are of $O(\mu^2)$.

The slow invariant manifold plays a fundamental role in trying to understand the qualitative changes of the dynamics as the stiff substructure of a coupled structure becomes more and more flexible. For sufficiently small coupling, the slow invariant manifold is a stable equilibrium for fast motions. However, as the coupling increases there will be interaction between the slow and fast dynamics. One mechanism that may cause such an interaction is the transverse intersection of the one-dimensional invariant manifolds to the saddle-centers. In this work, it has been shown that such an intersection generates stochastic dynamics. Another interaction may occur whenever a motion on the slow manifold loses stability transversely, through symmetry breaking and tangent bifurcations. This bifurcation could create periodic and stochastic motions residing in a higher-dimensional space and thus they activate fast oscillations.

A systematic methodology to study the dynamics of coupled structures has been presented. The methodology formulates the equations of motion as singular perturbation problems and introduces geometry through the concept of invariant manifolds to tackle the issues of dimension increases and dimension reduction in coupled structures. The singular perturbation formulation of the equations of motion presented here is universal since it models any linear one-dimensional

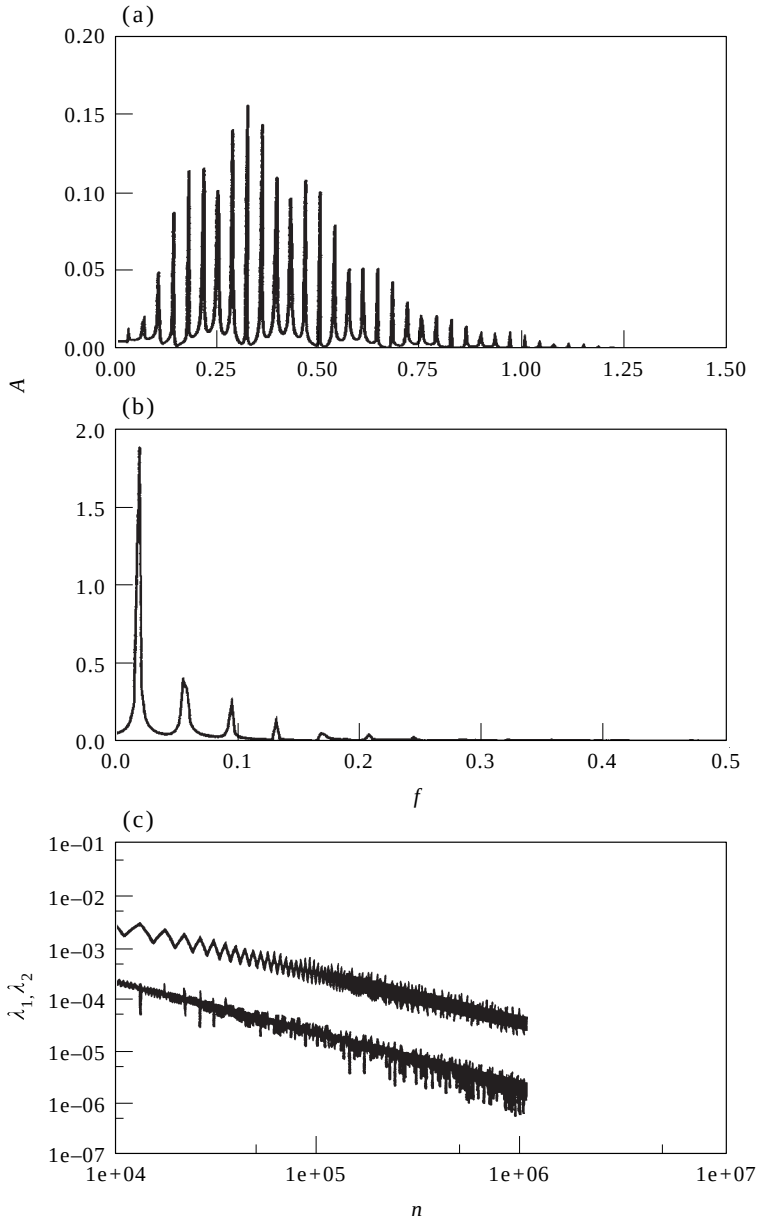

Figure 11. A near heteroclinic motion for weak coupling in the oscillator/pendulum system: (a) frequency spectrum of oscillator motion, (b) frequency spectrum of pendulum motion, (c) behavior of two Lyapunov characteristic exponents (1 075 200 iterates). System parameters: $\mu = 0{\cdot}001$, $\beta = 1$, $N = 1$.

continuum coupled to a planar pendulum oscillator. The methodology can be extended to model more complicated coupled structures as singular perturbation problems of properly chosen soft (low frequency) substructures.

ACKNOWLEDGMENT

The numerical computations were part of the DOD High Performance Computing (HPC) project "Dynamical modeling and control in large scale coupled structural and electronic systems". Ira Schwartz was supported by the Office of Naval Research.

REFERENCES

1. C. Lanzos 1986 *The Variational Principles of Mechanics*. New York: Dover.
2. J. Guckenheimer and P. Holmes 1982 *Nonlinear Oscillations, Dynamical Systems, and Bifurcations of Vector Fields*. New York: Springer.
3. S. Wiggins 1990 *Introduction to Applied Nonlinear Dynamical Systems and Chaos*. New York: Springer.
4. A. J. Lichtenberg and M. A. Lieberman 1992 *Regular and Chaotic Dynamics*. New York: Springer.
5. P. S. Landa 1996 *Nonlinear Oscillations and Waves in Dynamical Systems*. Boston, MA: Kluwer Academic.
6. L. Lui 1997 *Nonlinear Physics*. New York: Springer.
7. N. Fenichel 1979 *Journal of Differential Equations* **31**, 53–98. Geometric singular perturbation theory for ordinary differential equations.
8. H. W. Knobloch and B. Aulbach 1984 *Journal of Mathematical and Physical Sciences* **18**, 415–423. Singular perturbations and integral manifolds.
9. P. V. Kokotović, H. K. Khalil and J. O'Reilly 1986 *Singular Perturbation Methods in Control: Analysis and Design*. London: Academic Press.
10. I. T. Georgiou 1993 *Ph.D. Dissertation, Purdue University, West Lafayette, IN*. Nonlinear dynamics and chaotic motions of a singularly perturbed nonlinear viscoelastic beam.
11. I. T. Georgiou, A. K. Bajaj and M. Corless 1998 *International Journal of Non-Linear Mechanics* **33**, 275–300. Slow and fast invariant manifolds, and normal modes in a two-degree-of-freedom structural dynamical system with multiple equilibrium states.
12. I. T. Georgiou and I. B. Schwartz 1996 *International Journal of Bifurcation and Chaos* **6**, 673–692. The slow invariant manifold of a conservative pendulum–oscillator system.
13. I. T. Georgiou and I. B. Schwartz 1996 *ASME Journal of Applied Mechanics* **64**, 175–182. Slaving the in-plane motions of a nonlinear plate to its flexural motions: an invariant manifold approach.
14. R. M. Rosenberg 1964 *Quarterly of Applied Mathematics* **22**, 217–234. On the existence of normal mode vibrations of nonlinear systems with two degrees of freedom.
15. A. F. Vakakis, L. I. Manevitch, Yu. V. Mikhlin, V. N. Pilipchuck and A. A. Zevin 1996 *Normal Modes and Localization in Nonlinear Systems*. New York: Wiley Interscience.
16. S. W. Shaw and C. Pierre 1993 *Journal of Sound and Vibration* **164**, 85–124. Normal modes for nonlinear vibratory systems.
17. A. F. Vakakis 1994 *Journal of Sound and Vibration* **170**, 119–129. Exponentially small splittings of manifolds in a rapidly forced Duffing system.
18. P. Holmes, J. Marsden and J. Scheurle 1988 *Contemporary Mathematics* **81**, 213–244. Exponentially small splittings of separatrices with applications to KAM theory and degenerate bifurcations.
19. I. T. Georgiou and I. B. Schwartz 1997 *SIAM Journal on Applied Mathematics* (in press). Dynamics of large scale coupled structural/mechanical systems: a singular perturbation/proper orthogonal decomposition approach.

APPENDIX A: COUPLED OSCILLATORS

To apply the GSP theory one needs first to turn the ODE-PDE coupled system (3) into a set of coupled oscillators. The displacement can be decomposed,

$$V(\xi, \tau) = V_h(\xi, \tau) + v(\xi, \tau). \tag{A1}$$

$V_h(\xi, \tau)$ is the solution to the boundary value problem with homogeneous boundary conditions, i.e.,

$$\mu^2\pi^2\ddot{V}_h(\xi, \tau) = 4V_h''(\xi, \tau), \tag{A2a}$$

$$V_h(\xi = 0, \tau) = 0, \qquad V_h'(\xi = 1, \tau) = 0. \tag{A2b}$$

It is easy to show that

$$4v(\xi, \tau) = -\mu^2\beta\pi^2[1 - T\cos(\theta)]\xi.$$

The shapes of the spatial modes and the natural frequencies of the homogeneous boundary value problem (A2) are given by

$$\phi_m(\xi) = \sin\left(\frac{(2m-1)\pi}{2}\,\xi\right), \qquad \hat{\omega}_m^2 = \frac{(2m-1)^2}{\mu^2} = \frac{1}{\mu^2\mu_m^2}. \tag{A3}$$

The displacements in equation (43) are expanded:

$$V(\xi, \tau) = \sum_{m=1}^{\infty} \eta_m(\tau)\phi_m(\xi), \qquad V_h(\xi, \tau) = \sum_{m=1}^{\infty} \lambda_m(\tau)\phi_m(\xi),$$

$$v(\xi, \tau) = \sum_{m=1}^{\infty} \sigma_m(\tau)\phi_m(\xi). \tag{A4}$$

The PDE (3b) along with its boundary conditions is reduced to the following infinite set of oscillators:

$$\ddot{\eta}_m + \frac{\eta_m}{\mu^2\mu_m^2} + 2\beta(-1)^{m+1}\ddot{V}_A(\tau)\cos^2(\theta) + (-1)^m 2\beta[\sin^2(\theta) - \dot{\theta}^2\cos(\theta)] = 0, \tag{A5}$$

where

$$\ddot{V}_A(\tau) \equiv \sum_{m=1}^{\infty} \phi_m(\xi = 1)\ddot{\eta}_m(\tau) = \sum_{m=1}^{\infty} (-1)^{m+1}\ddot{\eta}_m(\tau). \tag{A6}$$

APPENDIX B: COMPUTATION OF THE SLOW MANIFOLD

Upon substituting series (19) into slow manifold condition (18), one obtains a recursive algorithm determining the expansion terms. Using computer algebra (code Maple), the approximation terms $\mathbf{H}^j$, $j = 1, 2, \ldots, 6$, have been computed

for the systems $N = 1, 2, 3, \ldots, 10$. The explicit dependence of the slow manifold on the order of truncation N was found in closed form. This result enables us to construct a slow manifold for the infinite system.

The expressions for the pair elements of the approximation terms are given below:

Term $\mathbf{H}^1$:

$$\{H^1_{2m-1}(\Psi), H^1_{2m}(\Psi)\} = (-1)^m 2\beta\{0, \sin(\Psi_1)\Psi_2[\Psi_2^2 + 4\cos(\Psi_1)]\}. \tag{B1}$$

Term $\mathbf{H}^2$:

$$\{H^2_{2m-1}(\Psi), H^2_{2m}(\Psi)\} = (-1)^m 2\beta\left\{\sum_{j=0}^{5} P_{jm2}(\Psi_2; \mu_m, N)\cos^j(\Psi_1), 0\right\}, \tag{B2}$$

where

$$P_{0m2}(\Psi_2; \mu_m, N) = 7\Psi_2^2\mu_m^2, \qquad P_{1m2}(\Psi_2; \mu_m, N) = (-\Psi_2^4 + 4)\mu_m^2,$$

$$P_{2m2}(\Psi_2; \mu_m, N) = (-11\mu_m^2 + 14\beta\sigma_1(N))\Psi_2^2,$$

$$P_{3m2}(\Psi_2; \mu_m, N) = -4\mu_m^2 + 8\beta\sigma_1(N) - 2\beta\sigma_1(N)\Psi_2^4,$$

$$P_{4m2}(\Psi_2; \mu_m, N) = -22\beta\sigma_1(N)\Psi_2^2, \qquad P_{5m2}(\Psi_2; \mu_m, N) = -8\beta\sigma_1(N).$$

Term $\mathbf{H}^3$:

$$\{H^3_{2m-1}(\Psi), H^3_{2m}(\Psi)\} = (-1)^m 2\beta\left\{\sin(\Psi_1)\Psi_2 \sum_{j=0}^{4} V_{jm3}(\Psi_2; \mu_m, N)\cos^j(\Psi_1), 0\right\}, \tag{B3}$$

where

$$V_{0m3}(\Psi_2; \mu_m, N) = \mu_m^2(\Psi_2^4 - 18),$$

$$V_{1m3}(\Psi_2; \mu_m, N) = (26\mu_m^2 - 56\beta\mu_m\sigma_1(N)\Psi_2^2),$$

$$V_{2m3}(\Psi_2; \mu_m, N) = 34\mu_m^2 - 68\beta\sigma_1(N) + 10\beta\sigma_1(N)\Psi_2^4,$$

$$V_{3m3}(\Psi_2; \mu_m, N) = 140\beta\sigma_1(N)\Psi_2^2, \qquad V_{4m3}(\Psi_2; \mu_m, N) = 100\beta\sigma_1(N).$$

The computations reveal that the expansion terms depend explicitly on the truncation order N through the following series of the rod frequency ratios μ_m:

$$\sigma_1(N) \equiv \sum_{m=1}^{N} \mu_m^2 = \sum_{m=1}^{N} \frac{1}{(2m-1)^2}.$$

Furthermore, they depend explicitly on the frequency ratios μ_m. High order approximations are computed to further explore how the approximation terms depend on the rod frequency ratios and the order of truncation.

Term $\mathbf{H}^4$:

$$\{H^4_{2m-1}(\Psi; N), H^4_{2m}(\Psi; N)\} = (-1)^m 2\beta \left\{ \sum_{j=0}^{8} P_{jm4}(\Psi_2; \mu_m, N) \cos^j(\Psi_1), 0 \right\}, \quad \text{(B4)}$$

where the various coefficients are given by

$$P_{0j4}(\Psi_2; \mu_m, N) = -18\mu_j^4 - (-31\mu_j^4 + 98\beta\mu_j^2\sigma_1(N))\Psi_2^4,$$

$$P_{1j4}(\Psi_2; \mu_m, N) = (164\mu_j^4 - 384\beta\mu_j^2\sigma_1(N))\Psi_2^2 + (-\mu_j^4 + 26\beta\mu_j^2\sigma_1(N))\Psi_2^6,$$

$$P_{2j4}(\Psi_2; \mu_m, N) = 52\mu_j^4 - 36\beta\sigma_2(N) - 100\beta\mu_j^2\sigma_1(N) + (-54\beta\mu_j^4 + 62\beta\sigma_2(N) + 698\beta\sigma_1(N) - 196\beta^2\sigma_1^2(N))\Psi_2^4,$$

$$P_{3j4}(\Psi_2; \mu_m, N) = (-180\mu_j^4 + 328\beta\sigma_2(N) + 1384\beta\mu_j^2\sigma_1(N) - 768\beta^2\sigma_1^2(N))\Psi_2^2 + (-2\beta\sigma_2(N) - 36\beta\mu_j^2\sigma_1(N) + 52\beta^2\sigma_1^2(N))\Psi_2^6,$$

$$P_{4j4}(\Psi_2; \mu_m, N) = -34\mu_j^4 + 104\beta\sigma_2(N) + 232\beta\mu_j^2\sigma_1(N) - 200\beta^2\sigma_1(N)^2 + (-114\beta\sigma_2^2(N) - 684\beta\mu_j^2\sigma_1(N) + 1396\beta^2\sigma_1^2(N))\Psi_2^4,$$

$$P_{5j4}(\Psi_2; \mu_m, N) = (-360\beta\sigma_2(N) - 1032\beta\mu_j^2\sigma_1(N) + 2768\beta^2\sigma_1^2(N))\Psi_2^2 - 72\beta^2\sigma_1^2(N)\Psi_2^4,$$

$$P_{6j4}(\Psi_2; \mu_m, N) = -68\beta\sigma_2(N) - 132\beta\mu_j^2\sigma_1(N) + 464\beta^2\sigma_1^2(N) - 1368\beta^2\sigma_1^2(N)\Psi_2^4,$$

$$P_{7j4}(\Psi_2; \mu_m, N) = -2064\beta^2\sigma_1^2(N)\Psi_2^2, \qquad P_{8j4}(\Psi_2; \mu_m, N) = -264\beta^2\sigma_1^2(N).$$

Term $\mathbf{H}_5$:

$$\{H^5_{2m-1}(\Psi; N), H^5_{2m}(\Psi; N)\} = (-1)^m 2\beta \times \left\{ 0, \sin(\Psi_1)\Psi_2 \sum_{j=0}^{7} V_{jm5}(\Psi_2; \mu_m, N) \cos^j(\Psi_1) \right\}. \quad \text{(B5)}$$

$$V_{0j5}(\Psi_2; \mu_m, N) = (288\mu_j^5 - 972\beta\mu_j^3\sigma_1(N))\Psi_2^2 + (-\mu_j^5 + 26\beta\mu_j^3\sigma_1(N))\Psi_2^6,$$

$$V_{1j5}(\Psi_2; \mu_m, N) = 432\mu_j^5 + \beta(-144\mu_j\sigma_2(N) - 1224\mu_j^5 - 1080\mu_j^3\sigma_1(N)), + (-120\mu_j^5 + \beta(284\sigma_2(N) + 1636\mu_j^3\sigma_1(N)) + \beta^2 784\mu_j\sigma_1^2(N))\Psi_2^4,$$

$$V_{2j5}(\Psi_2; \mu_m, N) = (-768\mu_j^5 + \beta(1888\mu_j\sigma_2(N) + 7592\mu_j^3\sigma_1(N) - \beta^2 5016\mu_j\sigma_1^2(N))\Psi_2^2 + \beta(-10\mu_j\sigma_2(N) - 116\mu_j^3\sigma_1(N) + \beta^2 260\mu_j\sigma_1^2(N))\Psi_2^6,$$

$$V_{3j5}(\Psi_2; \mu_m, N) = (-496\mu_j^5 + \beta(1280\mu_j\sigma_2(N) + 3984\mu_j^3\sigma_1(N) - \beta^2 2960\mu_j\sigma_1^2(N)) + \beta((-696\mu_j\sigma_2(N) - 3084\mu_j^3\sigma_1(N) + \beta^2 8856\mu_j\sigma_1^2(N)),$$

$$V_{4j5}(\Psi_2; \mu_m, N) = \beta(-1264\mu_j\sigma_2(N) - 3032\mu_j^3\sigma_1(N) + \beta^2 984\mu_j\sigma_1^2(N)) - \beta^2 11640\sigma_2^2(N)\Psi_2^4,$$

$$V_{5j5}(\Psi_2; \mu_m, N) = \beta(-1264\mu_j\sigma_2(N) - 3032\mu_j^3\sigma_1(N)) + 982\beta^2\mu_j\sigma_1^2(N) - 11640\beta^2\sigma_1^2(N)\Psi_2^4,$$

$$V_{6j5}(\Psi_2; \mu_m, N) = -25080\beta^2\mu_j\sigma_1^2(N), \qquad V_{7j5}(\Psi_2; \mu_m, N) = -7120\beta^2\mu_j\sigma_1^2(N).$$

Higher order approximation terms have the same structure. For instance, the $O(\mathbf{H}^6)$ has the following structure:

$$\{H^6_{2m-1}(\Psi; N), H^6_{2m}(\Psi; N)\} = (-1)^m 2\beta\left\{\sum_{j=0}^{12} P_{jm6}(\Psi_2, \mu_m, N)\cos^j(\Psi_1), 0\right\}. \quad \text{(B6)}$$

The coefficients depend explicitly on the order of truncation N through finite sequences of the normalized frequency μ_m:

$$\sigma_1(N) \equiv \sum_{m=1}^{N} \mu_m^2 = \sum_{m=1}^{N} \frac{1}{(2m-1)^2}, \qquad \sigma_2(N) \equiv \sum_{m=1}^{N} \mu_m^4 = \sum_{m=1}^{N} \frac{1}{(2m-1)^4},$$

$$\sigma_3(N) \equiv \sum_{m=1}^{N} \mu_m^6 = \sum_{m=1}^{N} \frac{1}{(2m-1)^6}.$$

Their limits are

$$\sigma_1 \equiv \lim_{N\to\infty} \sigma_1(N) = \frac{\pi^2}{8}, \qquad \sigma_2 \equiv \lim_{N\to\infty} \sigma_2(N) = \frac{\pi^4}{96}, \qquad \sigma_3 \equiv \lim_{N\to\infty} \sigma_3(N) = \frac{\pi^6}{960}.$$

Since these sequences converge, the low order approximations in μ to the slow manifold define corresponding low order approximations to the slow invariant manifold of the pendulum/flexible rod ($N = \infty$).

APPENDIX C: LINEARIZED SYSTEM

The coefficients of the linearization (42) of the oscillator/pendulum system (40) are given below

$$I_1^2(\Psi_1)J_{21} = -\cos(\Psi_1)(1 + 2\beta - \beta\cos^2(\Psi_1))Z_1 - \beta\Psi_2^2 - (1 + 3\beta + 2\beta^2)\cos(\Psi_1) + \beta(2 + \beta)\Psi_2^2\cos^2(\Psi_1) + \beta(1 + \beta)\cos^3(\Psi_1),$$

$$I_1(\Psi_1)J_{22} = \beta\Psi_2\sin(2\Psi_1), \qquad I_1(\Psi_1)J_{23} = -\sin(\Psi_1),$$

$$I_1^2(\Psi_1)J_{41} = -\beta\sin(2\Psi_1)Z_1 - \beta\Psi_2^2\sin(\Psi_1) - (\beta + 1)\sin(2\Psi_1) - \beta^2\Psi_2^2\sin(\Psi_1)\cos^2(\Psi_2),$$

$$I_1(\Psi_1)J_{42} = 2\beta\Psi_2\sin(\Psi_1), \qquad I_1(\Psi_1)J_{43} = -1.$$